INTERNATIONAL JOURNAL FOR NUMERICAL METHODS IN FLUIDS, VOL. 5, 25–42 (1985)

NUMERICAL CALCULATION OF EQUIVALENT MOMENT OF INERTIA FOR A FLUID IN A CYLINDRICAL CONTAINER WITH PARTITIONS

ILYA S. PARTOM

A.D.A., P.O.B. 2250 Haifa, Israel

SUMMARY

A 3-D numerical code was developed to solve the irrotational flow of an ideal fluid inside a moving cylindrical container with partitions. The problem is formulated in terms of two Poisson equations, the velocity equation and the pressure equation. These are expressed in terms of finite differences and solved by a procedure of line over relaxation. From the fluid pressure we computed the resultant moment on the container which was then expressed in terms of the equivalent moment of inertia. The code was checked against analytical results of Moiseyev and we found an agreement of 2–5 per cent even for a sparse mesh. We then demonstrated the capability of the code by computing the equivalent moment of inertia for various configurations with full and partial partitions.

KEY WORDS Fluid Sloshing Equivalent Moment of Inertia Partitioned Container Finite Differences Euler's Equations

INTRODUCTION

In an analysis of the fluid motion inside a moving container the following simplifying assumptions are often made:[1] rigid tank, ideal fluid, irrotational (potential) flow field. With these assumptions and for the case where the fluid completely fills the container, Zhukovskiy[2] proved that it is possible to replace the fluid body by an equivalent rigid body. Zhukovskiy also proved the following theorem, as stated in Reference 3. 'The ellipsoid of inertia of the equivalent body is always contained in the ellipsoid of inertia of the fluid'. Zhukovskiy also devised analytical methods to determine the moment of inertia of the equivalent bodies for containers of various geometries, e.g. ellipsoid, cylinder, cylinder with two, four or eight symmetrically spaced radial partitions, half a sphere, rectangular parallelepiped, etc. These analytical methods are effective for geometries with a certain amount of symmetry, but become intractable for complex geometries. For these, recourse to numerical methods is necessary. In this paper a numerical scheme is developed to solve the irrotational flow equations in cylindrical co-ordinates.[4] It is applied to a cylindrical container with various arrangements of symmetrical and non-symmetrical partitions, and the equivalent moment of inertia for these arrangements is calculated.

THEORY

Let the absolute velocity field of the fluid be denoted by $\mathbf{V}$. Then Euler's equations for the fluid motion are

$$\frac{\partial \mathbf{V}}{\partial t} + (\mathbf{V}\cdot\text{grad})\mathbf{V} = -\frac{1}{\rho}\text{grad}\, P \tag{1}$$

0271–2091/85/01 0025–18$01.80

Received 4 October 1983
Revised 1 March 1984

$$\operatorname{div}\mathbf{V} = 0 \tag{2}$$

where P is the pressure in the fluid and ρ is its mass density.

Let $\mathbf{V}_b$ denote the rigid body velocity field of the container. The velocity field of the fluid $\mathbf{U}$ relative to the container is given by

$$\mathbf{U} = \mathbf{V} - \mathbf{V}_b \tag{3}$$

As $\operatorname{div}\mathbf{V}_b = 0$ we have from equations (2) and (3) that also

$$\operatorname{div}\mathbf{U} = 0 \tag{4}$$

Expressing equation (1) in terms of the relative velocity $\mathbf{U}$ yields[5]

$$\frac{\partial \mathbf{U}}{\partial t} + (\mathbf{U}\cdot\operatorname{grad})\mathbf{U} = -\frac{1}{\rho}\operatorname{grad} P - \mathbf{A}_b - 2(\boldsymbol{\omega}\times\mathbf{U}) \tag{5}$$

where $\boldsymbol{\omega}$ is the angular velocity of the container, so that

$$\mathbf{V}_b = \mathbf{V} + \boldsymbol{\omega}\times\mathbf{R} \tag{6}$$

$\mathbf{R}$ is the radius vector to a point in the container.

$\mathbf{V}_0$ is the translation velocity.

$\mathbf{A}_b$ is the acceleration of the container given by

$$\mathbf{A}_b = \mathbf{A}_0 + \boldsymbol{\gamma}\times\mathbf{R} + \boldsymbol{\omega}\times(\boldsymbol{\omega}\times\mathbf{R}) \tag{7}$$

where $\mathbf{A}_0$ is the translation acceleration and $\boldsymbol{\gamma}$ is the angular acceleration of the container.

Taking the divergence of both sides of equation (5) and using equation (4) we have

$$\operatorname{div}\operatorname{grad} P = S_p(\mathbf{U}) \tag{8}$$

where

$$\mathbf{S}_p(\mathbf{U}) = -\rho\operatorname{div}[(\mathbf{U}\cdot\operatorname{grad})\mathbf{U} + \mathbf{A}_b + 2(\boldsymbol{\omega}\times\mathbf{U})] \tag{9}$$

We refer to equation (8) as the pressure equation. To solve for the flow field $\mathbf{U}$ we start from an initial flow field $\mathbf{U}_0$ given by

$$\mathbf{U}_0 = -\mathbf{V}_b \tag{10}$$

Generally $\mathbf{U}_0$ is not compatible with the boundary conditions, so that

$$\operatorname{div}\mathbf{U}_0 = S_u \neq 0 \tag{11}$$

The velocity field $\mathbf{U}$ that is compatible with the boundary conditions is given by

$$\mathbf{U} = \mathbf{U}_0 + \mathbf{U}_c \tag{12}$$

and from equations (4) and (11) we have

$$\operatorname{div}\mathbf{U}_c = -\operatorname{div}\mathbf{U}_0 = -S_u \tag{13}$$

By comparing equation (12) with equation (13) and using equation (10) we see that for irrotational flow $\mathbf{U}_c$ is derivable from a potential field ϕ:

$$\mathbf{U}_c = \operatorname{grad}\phi \tag{14}$$

Combining with equation (13) we have

$$\operatorname{div}\operatorname{grad}\phi = -S_u \tag{15}$$

We refer to equation (15) as the velocity equation.

As a result the problem is defined by two Poisson equations, the pressure equation (8) and the velocity equation (15) together with boundary conditions at the container walls and at both sides of partitions inside the fluid (see Figure 3).

The boundary condition for the velocity equation is

$$\frac{\partial \phi}{\partial n} = 0 \tag{16}$$

where n is the direction normal to the fluid boundary at the container walls or at the partitions.

The boundary condition for the pressure equation is

$$(\text{grad}\, P)_n = -\rho[(\mathbf{U}\cdot\text{grad})\mathbf{U} + \mathbf{A}_b + 2(\boldsymbol{\omega} \times \mathbf{U})]_n \tag{17}$$

To construct the numerical scheme we first express the governing equations (8) and (15) and the boundary conditions (16) and (17) in terms of cylindrical co-ordinates (r, θ, z) attached to the cylindrical container. For this we use the following notation:

$$\mathbf{F} = \mathbf{A}_b + 2(\boldsymbol{\omega} \times \mathbf{U}) \tag{18}$$

$$\mathbf{T} = (\mathbf{U}\cdot\text{grad})\mathbf{U} \tag{19}$$

We thus have

$$\left.\begin{aligned} F_r &= 2(\omega_\theta u_z - \omega_z u_\theta) - r(\omega_\theta^2 + \omega_z^2) + z(\omega_r\omega_z + \gamma_\theta) + a_{0_r} \\ F_\theta &= 2(\omega_z u_r - \omega_r u_z) + r(\omega_r\omega_\theta + \gamma_z) + z(\omega_\theta\omega_z - \gamma_r) + a_{0_\theta} \\ F_z &= 2(\omega_r u_\theta - \omega_\theta u_r) + r(\omega_r\omega_z - \gamma_\theta) - z(\omega_r^2 + \omega_\theta^2) + a_{0_z} \end{aligned}\right\} \tag{20}$$

$$\left.\begin{aligned} T_r &= \frac{1}{r}\frac{\partial}{\partial r}(ru_r^2) + \frac{1}{r}\frac{\partial}{\partial \theta}(u_r u_\theta) + \frac{\partial}{\partial z}(u_r u_z) - \frac{1}{r}u_\theta^2 \\ T_\theta &= \frac{1}{r}\frac{\partial}{\partial r}(ru_r u_\theta) + \frac{1}{r}\frac{\partial}{\partial \theta}(u_\theta^2) + \frac{\partial}{\partial z}(u_\theta u_z) + \frac{1}{r}u_r u_\theta \\ T_z &= \frac{1}{r}\frac{\partial}{\partial r}(ru_r u_z) + \frac{1}{r}\frac{\partial}{\partial \theta}(u_\theta u_z) + \frac{\partial}{\partial z}(u_z^2) \end{aligned}\right\} \tag{21}$$

where

u_r, u_θ, u_z are the component of $\mathbf{U}$

$\omega_r, \omega_\theta, \omega_z$ are the component of $\boldsymbol{\omega}$

$a_{0_r}, a_{0_\theta}, a_{0_z}$ are the component of $\mathbf{A}_0$

$$-\frac{1}{\rho}S_p = \frac{1}{r}\frac{\partial}{\partial r}[r(T_r + F_r)] + \frac{1}{r}\frac{\partial}{\partial \theta}(T_\theta + F_\theta) + \frac{\partial}{\partial z}(T_z + F_z) \tag{22}$$

and the pressure equation is

$$\frac{1}{r}\frac{\partial}{\partial r}\left(r\frac{\partial P}{\partial r}\right) + \frac{1}{r^2}\frac{\partial^2 P}{\partial \theta^2} + \frac{\partial^2 P}{\partial z^2} = S_p \tag{23}$$

The pressure boundary conditions are

$$\frac{\partial P}{\partial n} = -\rho(T_n + F_n) \tag{24}$$

The velocity equation is

$$\frac{1}{r}\frac{\partial}{\partial r}\left(r\frac{\partial \phi}{\partial r}\right) + \frac{1}{r^2}\frac{\partial^2 \phi}{\partial \theta^2} + \frac{\partial^2 \phi}{\partial z^2} = S_u \tag{25}$$

NUMERICAL SOLUTION

To construct the difference equations we embed into the cylindrical cavity a 3-D cylindrical network as shown in Figure 1. The cells of the network are formed by radial planes, horizontal planes and cylindrical surfaces. The container walls coincide with net cell boundaries. Whenever there are rigid partitions inside the fluid they also coincide with cell boundaries.

In some cases a rigid axial rod of diameter d in the centre of the container has been considered. In these cases the outer surface of the rod coincides with the boundaries of the innermost cells.

Referring to Figure 1 we denote the cells by (i,j,k) corresponding to the (r,θ,z) directions. The numbers of cells in each direction are

$$i = 1,\cdots,m \qquad j = 1,\cdots,n \qquad k = 1,\cdots,l \tag{26}$$

The pressure P and the potential function ϕ are defined at cell centres. Referring once more to Figure 1 we denote the inner, front and lower faces of the (i,j,k) cell by (i,j,k), respectively. The

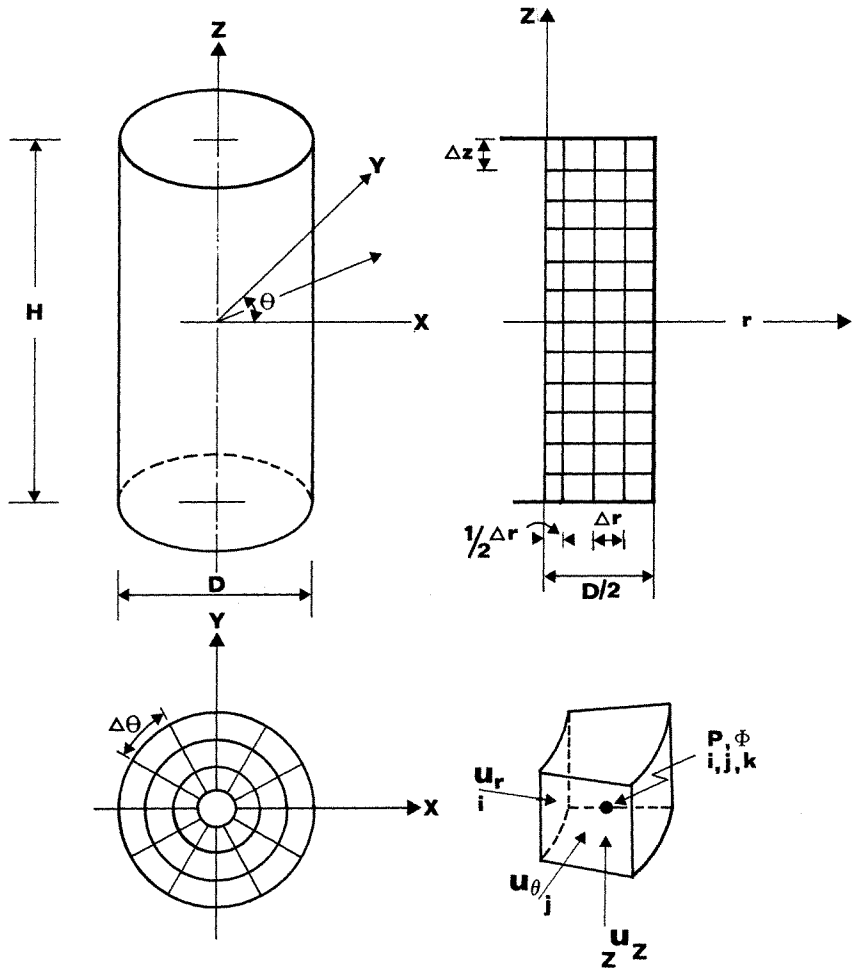

Figure 1. Container and mesh geometry

components of the velocity vector (u_r, u_θ, u_z) are defined at the (i,j,k) cell faces so that we have a staggered 3-D network.

The size of each cell is $(\Delta r, \Delta\theta, \Delta z)$, where

$$\left.\begin{aligned} \Delta r &= \frac{D-d}{2m}; \quad \text{with an axial rod} \\ \Delta r &= \frac{D}{2m+1}; \quad \text{no axial rod} \\ \Delta\theta &= 2\pi/n \\ \Delta z &= H/l \end{aligned}\right\} \tag{27}$$

The right hand sides of equations (8) and (15) are divergences of vectors. Their finite difference approximations are given by

$$\begin{aligned} \operatorname{div}\mathbf{f} \simeq{}& \frac{1}{r(i+\frac{1}{2})}\frac{1}{\Delta r}[r(i+1)f_r(i+1,j,k) - r(i)f_r(i,j,k)] \\ &+ \frac{1}{r(i+\frac{1}{2})}\frac{1}{\Delta\theta}[f_\theta(i,j+1,k) - f_\theta(i,j,k)] + \frac{1}{\Delta z}[f_z(i,j,k+1) - f_z(i,j,k)] \end{aligned} \tag{28}$$

where $\mathbf{f}$ is $\mathbf{U}_0$ for S_u and $\mathbf{T}+\mathbf{F}$ for S_p.

For writing down the finite difference approximations of the components of $\mathbf{T}$ and $\mathbf{F}$ we first define

$$\left.\begin{aligned} T_r &= T_{rr} + T_{r\theta} + T_{rz} \\ T_\theta &= T_{\theta r} + T_{\theta\theta} + T_{\theta z} \\ T_z &= T_{zr} + T_{z\theta} + T_{zz} \end{aligned}\right\} \tag{29}$$

$$\left.\begin{aligned} F_r &= F_{rr} + F_{r\theta} + F_{rz} \\ F_\theta &= F_{\theta r} + F_{\theta\theta} + F_{\theta z} \\ F_z &= F_{zr} + F_{z\theta} + F_{zz} \end{aligned}\right\} \tag{30}$$

The finite difference approximations are:

$$\left.\begin{aligned} T_{rr} &= \frac{1}{r}\frac{\partial}{\partial r}(ru_r^2) \simeq \frac{1}{r(i)}\frac{1}{2\Delta r}[r(i+1)u_r^2(i+1,j,k) - r(i-1)u_r^2(i-1,j,k)] \\ T_{r\theta} &= \frac{1}{r}\left[\frac{\partial}{\partial\theta}(u_r u_\theta) - u_\theta^2\right] \simeq \frac{1}{r(i)}\left\{\frac{1}{\Delta\theta}[u_r(i,j+\tfrac{1}{2},k)u_\theta(i-\tfrac{1}{2},j+1,k)\right. \\ &\qquad \left. - u_r(i,j-\tfrac{1}{2},k)u_\theta(i-\tfrac{1}{2},j,k)] - u_\theta^2(i-\tfrac{1}{2},j+\tfrac{1}{2},k)\right\} \\ T_{rz} &= \frac{\partial}{\partial z}(u_r u_z) \simeq \frac{1}{\Delta z}[u_r(i,j,k+\tfrac{1}{2})u_z(i-\tfrac{1}{2},j,k+1) - u_r(i,j,k-\tfrac{1}{2})u_z(i-\tfrac{1}{2},j,k)] \end{aligned}\right\} \tag{31}$$

where the half integer indices have the meaning as in

$$u_r(i,j+\tfrac{1}{2},k) = \tfrac{1}{2}[u_r(i,j+1,k) + u_r(i,j,k)] \tag{32}$$

$$
\left.\begin{aligned}
T_{\theta r} &= \frac{1}{r}\frac{\partial}{\partial r}(ru_r u_\theta) \simeq \frac{1}{r(i+\frac{1}{2})}\frac{1}{\Delta r}[r(i+1)u_r(i+1,j-\tfrac{1}{2},k)u_\theta(i+\tfrac{1}{2},j,k) \\
&\quad - r(i)u_r(i,j-\tfrac{1}{2},k)u_\theta(i-\tfrac{1}{2},j,k)] \\
T_{\theta\theta} &= \frac{1}{r}\left(\frac{\partial}{\partial\theta}u_\theta^2 + u_r u_\theta\right) \\
&\simeq \frac{1}{r(i+\frac{1}{2})}\left\{\frac{1}{\Delta\theta}[u_\theta^2(i,j+\tfrac{1}{2},k) - u_\theta^2(i,j-\tfrac{1}{2},k)] + u_r(i+\tfrac{1}{2},j-\tfrac{1}{2},k)u_\theta(i,j,k)\right\} \\
T_{\theta z} &= \frac{\partial}{\partial z}(u_\theta u_z) \simeq \frac{1}{\Delta z}[u_\theta(i,j,k+\tfrac{1}{2})u_z(i,j-\tfrac{1}{2},k+1) - u_\theta(i,j,k-\tfrac{1}{2})u_z(i,j-\tfrac{1}{2},k)]
\end{aligned}\right\} \tag{33}
$$

$$
\left.\begin{aligned}
T_{zr} &= \frac{1}{r}\frac{\partial}{\partial r}(ru_r u_z) \simeq \frac{1}{r(i+\frac{1}{2})}\frac{1}{\Delta r}[r(i+1)u_r(i+1,j,k-\tfrac{1}{2})u_z(i+\tfrac{1}{2},j,k) \\
&\quad - r(i)u_r(i,j,k-\tfrac{1}{2})u_z(i-\tfrac{1}{2},j,k)] \\
T_{z\theta} &= \frac{1}{r}\frac{\partial}{\partial\theta}(u_\theta u_z) \simeq \frac{1}{r(i+\frac{1}{2})}\frac{1}{\Delta\theta}[u_\theta(i,j+1,k-\tfrac{1}{2})u_z(i,j+\tfrac{1}{2},k) - u_\theta(i,j,k-\tfrac{1}{2})] \\
T_{zz} &= \frac{\partial}{\partial z}(u_z^2) \simeq \frac{1}{\Delta z}[u_z^2(i,j,k+\tfrac{1}{2}) - u_z^2(i,j,k-\tfrac{1}{2})]
\end{aligned}\right\} \tag{34}
$$

$$
\left.\begin{aligned}
F_{rr} &= 2(\omega_\theta u_z - \omega_z u_\theta) + a_{0_r} \\
&\simeq 2\{\omega_\theta[\theta(j+\tfrac{1}{2})]u_z(i-\tfrac{1}{2},j,k+\tfrac{1}{2}) - \omega_z u_\theta(i-\tfrac{1}{2},j+\tfrac{1}{2},k)]\} + a_{0_r} \\
F_{r\theta} &= -r(\omega_\theta^2 + \omega_z^2) \simeq -r(i)\{\omega_\theta^2[\theta(j+\tfrac{1}{2})] + \omega_z^2\} \\
F_{rz} &= z(\omega_r\omega_z + \gamma_\theta) \simeq z(k+\tfrac{1}{2})\{\omega_r[\theta(j+\tfrac{1}{2})]\omega_z - \gamma_\theta[\theta(j+\tfrac{1}{2})]\}
\end{aligned}\right\} \tag{35}
$$

where the components of $\boldsymbol{\omega}$ as well as the components of $\mathbf{A}_0, \mathbf{V}_0, \boldsymbol{\gamma}$ are computed from their Cartesian components by

$$
\left.\begin{aligned}
\omega_r &= \omega_x\cos\theta + \omega_y\sin\theta \\
\omega_\theta &= -\omega_x\sin\theta + \omega_y\cos\theta \\
\omega_z &= \omega_z
\end{aligned}\right\} \tag{36}
$$

$$
\left.\begin{aligned}
F_{\theta r} &= 2(\omega_z u_r - \omega_r u_z) + a_{0_\theta} \\
&\simeq 2[\omega_z u_r(i+\tfrac{1}{2},j-\tfrac{1}{2},k) - \omega_r[\theta(j)]u_z(i,j,k+\tfrac{1}{2})] + a_{0_\theta}[\theta(j)] \\
F_{\theta\theta} &= r(\omega_r\omega_\theta + \gamma_z) \simeq r(i+\tfrac{1}{2})[\omega_r[\theta_r[\theta(j)]\omega_\theta[\theta(j)] + \gamma_z \\
F_{\theta z} &= z(\omega_\theta\omega_z - \gamma_r) \simeq z(k+\tfrac{1}{2})[\omega_\theta[\theta(j)]\omega_z - \gamma_r[\theta(j)]
\end{aligned}\right\} \tag{37}
$$

$$
\left.\begin{aligned}
F_{zr} &= 2(\omega_r u_\theta - \omega_\theta u_r) + a_{0_z} \\
&\simeq 2\{\omega_r[\theta(j+\tfrac{1}{2})u_\theta(i,j+\tfrac{1}{2},k-\tfrac{1}{2}) - \omega_\theta[\theta(j+\tfrac{1}{2})]u_r(i+\tfrac{1}{2},j,k+\tfrac{1}{2}) + a_{0_z} \\
F_{z\theta} &= r(\omega_r\omega_z - \gamma_\theta) \simeq r(i+\tfrac{1}{2})\{\omega_r[\theta(j+\tfrac{1}{2})\omega_z - \gamma_\theta[\theta(j+\tfrac{1}{2})]\} \\
F_{zz} &= -z(\omega_r^2 + \omega_\theta^2) \simeq -z(k)\{\omega_r^2[\theta(j+\tfrac{1}{2})] + \omega_\theta^2[\theta(j+\tfrac{1}{2})]\}
\end{aligned}\right\} \tag{38}
$$

The finite difference approximations for the Poisson equations, (8) and (15), for a regular cell are

$$
\frac{1}{r(i+\frac{1}{2})}\frac{1}{\Delta r^2}\{r(i+1)[P(i+1,j,k) - P(i,j,k)] - r(i)[P(i,j,k) - P(i-1,j,k)]\}
$$

$$+\frac{1}{r^2(i+\frac{1}{2})}\frac{1}{\Delta\theta^2}[P(i,j-1,k)-2P(i,j,k)+P(i,j+1,k)]$$

$$+\frac{1}{\Delta z^2}[P(i,j,k-1)-2P(i,j,k)+P(i,j,k+1)]=S_p(i,j,k) \tag{39}$$

$$\frac{1}{r(i+\frac{1}{2})}\frac{1}{\Delta r^2}\{r(i+1)[\phi(i+1,j,k)-\phi(i,j,k)]-r(i)[\phi(i,j,k)-\phi(i-1,j,k)]\}$$

$$+\frac{1}{r^2(i+\frac{1}{2})}\frac{1}{\Delta\theta^2}[\phi(i,j-1,k)-2\phi(i,j,k)+\phi(i,j+1,k)]$$

$$+\frac{1}{\Delta z^2}[\phi(i,j,k-1)-2\phi(i,j,k)+\phi(i,j,k+1)]=-S_u(i,j,k) \tag{40}$$

As described before we have along the container axis, in the case without an axial rod, cylindrical cells with diameter Δr.

At the centre $r=0$ and the differential equations as well as the difference equations become singular. To avoid this problem we represent the velocity vector (as well as other vectors) by its Cartesian components u_x, u_y, u_z.

To devise the difference equations for the cylindrical cell we make use of the Gauss theorem for the divergence of a vector, namely:

$$\int_{\text{vol}} \operatorname{div}\mathbf{f}\,\mathrm{d}(\text{vol})=\oint\mathbf{f}\cdot\mathrm{d}\mathbf{S} \tag{41}$$

where $\mathbf{S}$ is the outer surface vector of the cylindrical cell.

The finite difference approximation of equation (41) is

$$\operatorname{div}\mathbf{f}(k)=\sum_{j=1}^{n} f_r(1,j,k)S_r/n+[f_z(k+1)-f_z(k)]S_z \tag{42}$$

where

$$\begin{aligned} S_r&=\frac{1}{n}\pi\Delta r\Delta z\\ S_r&=\tfrac{1}{4}\pi\Delta r^2 \end{aligned} \tag{43}$$

The finite difference approximations of the pressure equation and velocity equation are similarly given by

$$\sum_{j=1}^{n}[P(1,j,k)-P_c(k)]S_r/n+[P_c(k-1)-2P_c(k)+P_c(k+1)]S_z=S_p(k) \tag{44}$$

$$\sum_{j=1}^{n}[P(1,j,k)-\phi_c(k)]S_r/n+[\phi_c(k-1)-2\phi_c(k)+\phi_c(k+1)]S_z=-S_u(k) \tag{45}$$

where the index c refers to the value at the centre of a cylindrical cell.

The difference equations representing the pressure equation and the velocity equation together with boundary conditions (which are given by the derivative normal to the boundaries) constitute systems of N linear equations where N is the number of cells. To solve the linear systems we first tried the Gauss–Seidel elimination procedure with over-relaxation. We obtained a very slow convergence especially for configurations with partitions. To speed up convergence we used line relaxation along lines parallel to the z-axis.

For the velocity equation (40), we define

$$\left.\begin{aligned} C_a &= \frac{r(i+1)}{r(i+\frac{1}{2})}\frac{1}{\Delta r^2} \\ C_b &= \frac{r(i)}{r(i+\frac{1}{2})}\frac{1}{\Delta r^2} \\ C_c &= \frac{1}{r^2(i+\frac{1}{2})}\frac{1}{\Delta\theta^2} \end{aligned}\right\} \tag{46}$$

$$C_d = 1/\Delta z^2$$

$$C_f = -C_a - C_b + 2C_c + 2C_d$$

and retaining only the terms with the indices i, j on the left hand side we get:

$$\begin{aligned} &-C_d\phi(i,j,k-1) + C_f\phi(i,j,k) - C_d\phi(i,j,k+1) = -S_u(i,j,k) \\ &+C_a\phi(i+1,j,k) + C_b\phi(i-1,j,k) + C_c[\phi(i,j+1,k) + \phi(i,j-1,k)] \end{aligned} \tag{47}$$

Equation (47) is a tri-diagonal linear system of equations which can be solved by a very efficient and well-known algorithm. The boundary conditions $\partial\phi/\partial n = 0$ are expressed by

$$\phi_{in} = \phi_{out} \tag{48}$$

where ϕ_{in} is the value of ϕ in a cell next to the boundary (on the inside), and ϕ_{out} is the value of ϕ in a virtual cell outside the boundary. Equation (47) is altered at the boundaries as a result of equation (48). This is done by omitting one of the terms on the right hand side of equation (47) and correcting the coefficient C_f accordingly.

Near the cylindrical wall we have, for instance

$$\begin{aligned} &-C_d\phi(i,j,k-1) + C_{f_1}\phi(i,j,k) - C_d\phi(i,j,k+1) = -S_u(i,j,k) \\ &+C_d\phi(i-1,j,k) + C_c[\phi(i,j+1,k) + \phi(i,j-1,k)] \\ &C_{f_1} = C_f - C_a \end{aligned} \tag{49}$$

and similarly modified equations for the other boundaries.

The pressure equation is given by

$$\begin{aligned} &-C_dP(i,j,k-1) - C_fP(i,j,k) + C_dP(i,j,k+1) = S_p(i,j,k) \\ &-C_aP(i+1,j,k) - C_bP(i-1,j,k) - C_c[P(i,j-1,k) + P(i,j+1,k)] \end{aligned} \tag{50}$$

For a line of cells parallel to the z-axis this also is a tri-diagonal system of linear equations. The boundary conditions are given by

$$P_{out} = P_{in} \pm \frac{\partial P}{\partial n}\cdot\Delta n \tag{51}$$

where the sign is plus or minus according to whether the outer normal to the boundary is in the positive or negative direction of the appropriate co-ordinate axis, and where

$$\Delta n \equiv \Delta r,\ r\Delta\theta \quad \text{or} \quad \Delta z \tag{52}$$

Whenever the cell (i, j, k) is near a boundary, equation (50) is modified as a result of equation (51). Depending on the type of boundary one of the terms on the right hand side is replaced by $\pm\,\partial P/\partial n\cdot\Delta n$ and C_f is modified accordingly. For a cell near the container cylindrical wall, for

instance, the modified equation is

$$C_d P(i,j,k-1) - C_{f_1} P(i,j,k) + C_d P(i,j,k+1) = S_p(i,j,k)$$
$$- C_a \frac{\partial P}{\partial r}(m+1,j,k)\Delta r - C_b P(i-1,j,k) - C_c[P(i,j+1,k) + P(i,j-1,k)] \tag{53}$$
$$C_{f_1} = C_f + C_a$$

The line relaxation procedure is carried out by scanning lines of cells parallel to the z direction (including the line of cylindrical cells in the centre). For each line we assume that the values of the unknowns in neighbouring lines are known and we solve the tri-diagonal system. We also employ an over-relaxation coefficient α to speed convergence. By trials an optimal value of 1·8 for α was found.

As the boundary conditions in both Poisson equations are given by the normal derivative, adding a constant to the solution gives another proper solution. As a result the relaxation procedure tends to be unstable so that the mean value of the function grows monotonically. To avoid this one has to anchor the solution somehow. For the velocity equation we did this by setting $\phi = 0$ at one of the cells. For the pressure equation we anchor the solution in a way that ensures a positive pressure in all the cells. This was done by subtracting, after each scan, the lowest value of P in the net from the values of P in all the cells.

RESULTANT FORCE AND MOMENT

From the solution described in the previous section we obtain the velocity field $\mathbf{U}(i,j,k)$ and the pressure field $P(i,j,k)$. But of practical importance are the values of the resultant force $\mathbf{Q}$ and the resultant moment $\mathbf{M}$ (with respect to the origin, for example) that the fluid exerts on the container walls. From the resultant moment one can then deduce the equivalent moment of inertia.

To compute $\mathbf{Q}$ and $\mathbf{M}$ from the pressure field, the pressure from the mid cells near the boundary is first extrapolated to the boundaries by

$$P_b = P_{cell} \pm \frac{\partial P}{\partial n}\frac{\Delta n}{2} \tag{54}$$

where the sign depends on whether the outer normal to the boundary is in the direction of the axis (r, θ or z) at that point, and Δn is Δr, $r\Delta\theta$ or Δz.

For a boundary where $\mathbf{n}$ is in the radial direction the components of $\mathbf{Q}$ are given by

$$\left.\begin{aligned}(Q_x)_r &= 2\arcsin\frac{\Delta\theta}{2}\Delta z \sum_j \sum_k P_b(j,k)\cos\theta(j+\tfrac{1}{2}) \\ (Q_y)_r &= 2\arcsin\frac{\Delta\theta}{2}\Delta z \sum_i \sum_k P_b(j,k)\sin\theta(j+\tfrac{1}{2}) \\ (Q_z)_r &= 0\end{aligned}\right\} \tag{55}$$

where a is the radius of that boundary and the summations are over all the cells near that boundary.

For a boundary in the θ direction the components are

$$\left.\begin{aligned}(Q_x)_\theta &= -\Delta r\Delta z \sum_i \sum_k P_b(i,k)\cos\theta(j) \\ (Q_y)_\theta &= \Delta r\Delta z \sum_i \sum_k P_b(i,k)\sin\theta(j) \\ (Q_z)_\theta &= 0\end{aligned}\right\} \tag{56}$$

where the summations are over the cells near that boundary.

For a boundary in the z direction the components are

$$(Q_x)_z = (Q_y)_z = 0$$
$$(Q_z)_z = S_z P_c(k) + \Delta r \Delta\theta \sum_i \sum_j r(i+\tfrac{1}{2}) P_b(i,j) \tag{57}$$

where the first term in equation (57) is the contribution from the cylindrical cells, and the summation is over all the cells near that boundary.

Whenever the direction of **n** is in opposite sense to that of the relevant axis (r, θ or z) a minus sign has to be put in the corresponding equations for Q_x, Q_y and Q_z. The components of **Q** are finally given by:

$$\left.\begin{aligned} Q_x &= \sum (Q_x)_r + \sum (Q_x)_\theta \\ Q_y &= \sum (Q_y)_r + \sum (Q_y)_\theta \\ Q_z &= \sum (Q_z)_z \end{aligned}\right\} \tag{58}$$

where the summations are over all the boundaries (container boundaries, inner rod and partitions).

The resultant moment exerted by fluid on the container is given by

$$\mathbf{M} = \sum P_b \mathrm{d}\mathbf{S} \times \mathbf{R}_b \tag{59}$$

where the summation is over all of the boundary cells, where $\mathrm{d}\mathbf{S}$ is the vector of boundary cell face at the boundary, and where $\mathbf{R}_b$ is the boundary radius vector.

In Cartesian co-ordinates the vector product is

$$\mathbf{S} \times \mathbf{R}_b = 1_x(S_y z_b - S_z y_b) + 1_y(S_z x_b - S_x z_b) + 1_z(S_x y_b - S_y x_b) \tag{60}$$

Using this, the components of **M** are:

$$\left.\begin{aligned} (M_x)_r &= 2 \arcsin \frac{\Delta\theta}{2} \Delta z \sum_j \sum_k P_b(j,k) \sin\theta(j+\tfrac{1}{2}) z(k+\tfrac{1}{2}) \\ (M_y)_r &= -2 \arcsin \frac{\Delta\theta}{2} \Delta z \sum_i \sum_j P_b(j,k) \cos\theta(j+\tfrac{1}{2}) z(k+\tfrac{1}{2}) \\ (M_z)_r &= 0 \end{aligned}\right\} \tag{61}$$

$$\left.\begin{aligned} (M_x)_\theta &= \Delta r \Delta z \sum_i \sum_j P_b(i,k) \cos\theta(j) \Delta z(k+\tfrac{1}{2}) \\ (M_y)_\theta &= \Delta r \Delta z \sum_i \sum_k P_b(i,k) \sin\theta(j) \Delta z(k+\tfrac{1}{2}) \\ (M_z)_\theta &= -\Delta r \Delta z \sum_i \sum_k P_b(i,k) r(i+\tfrac{1}{2}) \end{aligned}\right\} \tag{62}$$

$$\left.\begin{aligned} (M_x)_z &= -\Delta r \Delta\theta \sum_i \sum_j P_b(i,j) r^2(i+\tfrac{1}{2}) \sin\theta(j+\tfrac{1}{2}) \\ (M_y)_z &= \Delta r \Delta\theta \sum_i \sum_j P_b(i,j) r^2(i+\tfrac{1}{2}) \cos\theta(j+\tfrac{1}{2}) \\ (M_z)_z &= 0 \end{aligned}\right\} \tag{63}$$

where the summations and notations are equivalent to those in the equations for the components of **Q**.

Finally we have

$$\left.\begin{aligned} M_x &= \sum(M_x)_r + \sum(M_x)_\theta + \sum(M_x)_z \\ M_y &= \sum(M_y)_r + \sum(M_y)_\theta + \sum(M_y)_z \\ M_z &= \sum(M_z)_\theta \end{aligned}\right\} \tag{64}$$

RESULTS AND DISCUSSION

Before computing the equivalent moment of inertia of various container configurations a series of runs to check the accuracy of the code was carried out. Even for a sparse mesh ($m = 3, n = 8, l = 20$ for $H/D = 4$) the accuracy of the pressure field was better than 5 per cent, as compared with the analytical solution. Consequently, and in order to save computer time, a sparse mesh was used in all subsequent computations.

To further check the code we made computations for a container without partitions and without an axial rod rotating around the x-axis. The container motion was $\boldsymbol{\omega} = (0, 0, 0)$ and $\boldsymbol{\gamma} = (1, 0, 0)$. We made these runs for containers with different aspect ratios H/D. For all the runs the integral results were: $\mathbf{Q} = (0, 0, 0)$, $\mathbf{M} = (M_x, 0, 0)$. The equivalent moment of inertia $(I_E)_x$ can then be obtained by

$$(I_E)_x = M_x/\gamma_x = M_x/1 \tag{65}$$

The analytical solution for $(I_E)_x$ as given in Reference 3 is

$$(I_E)_x = (I_E)_y = m_f\left(\frac{a^2}{4} + \frac{h^2}{3}\right) - m_f a^2\left[1 - 8\frac{a}{h}\sum_{n=1}^{\infty}\frac{1}{\xi_n^3(\xi^2 - 1)}\operatorname{tngh}\left(\xi_n\frac{h}{a}\right)\right] \tag{66}$$

where $a = D/2$, $h = H/2$, $m_f = \rho\pi\dfrac{D^2}{4}H$ is the fluid mass, and ξ_n are the roots of the equation

$$\frac{\mathrm{d}J_1(\xi)}{\mathrm{d}\xi} = 0 \tag{67}$$

where J_1 is the ordinary Bessel function of the first order.

To compare the numerical and analytical results $(I_E)_x$ is divided by the rigid body moment of inertia I_x, given by

$$I_x = m_f\left(\frac{D^2}{16} + \frac{H^2}{16}\right) \tag{68}$$

Table I. Relative equivalent moment of inertia, for a cylindrical container without partitions. Comparison between analytical and numerical solutions

H/D	$(I_E)_x/I_x$ analytical	numerical
1	0·1639	0·1744
1·5	0·3562	0·3608
2	0·5382	0·5392
3	0·7476	0·7462
4	0·8542	0·8429

The results are compared in Table I and Figure 2. We see that the agreement is better than 2 per cent. A much better agreement can undoubtedly be obtained with a denser mesh.

The next configuration we computed was a cylindrical container with different number of symmetrically spaced longitudinal partitions, rotating around the z-axis. For such configurations

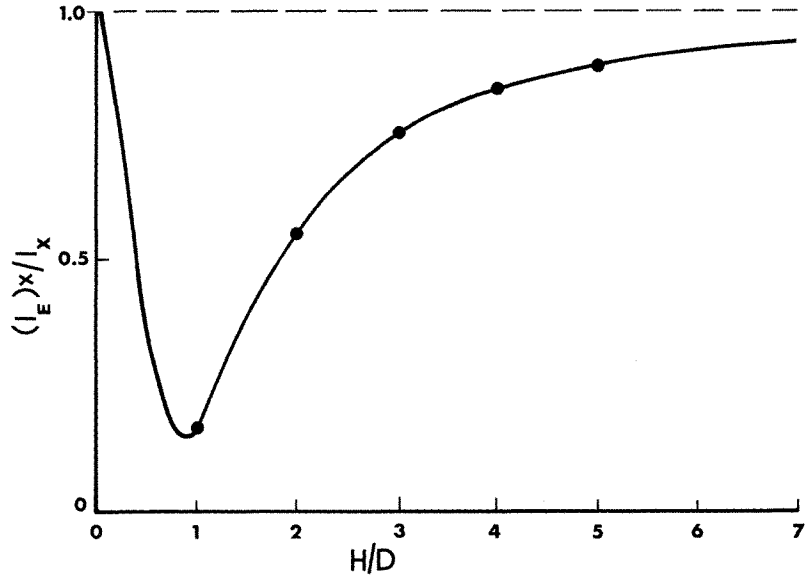

Figure 2. The relative equivalent moment of inertia for a full cylindrical container as a function of the aspect ratio. Full line: analytical solution: Points: numerical solution

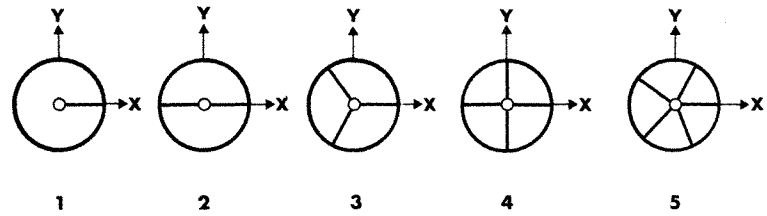

Figure 3. Cross-sections of the five configurations of cylindrical containers with partitions

Table II. Cylindrical container with symmetrically spaced longitudinal partitions. Comparison between numerical and analytical solutions

Number of partitions	$(I_E)_z/I_z$ numerical	analytical
0	0	0
1	0·5596	—
2	0·6538	0·622
3	0·7460	—
4	0·8084	0·790
5	0·8561	—
8	0·9287	0·9081

results for $(I_E)_z/I_z$ based on an analytical solution, for 2, 4 and 8 partitions are given in Reference 3. Our computations were for configurations having from 1 to 8 partitions. The different configurations are shown in Figure 3.

The results for $(I_E)_z/I_z$ are given in Table II and Figure 4. We see that for the cases where there is an analytical result the difference from our numerical results is within 5 per cent. The difference

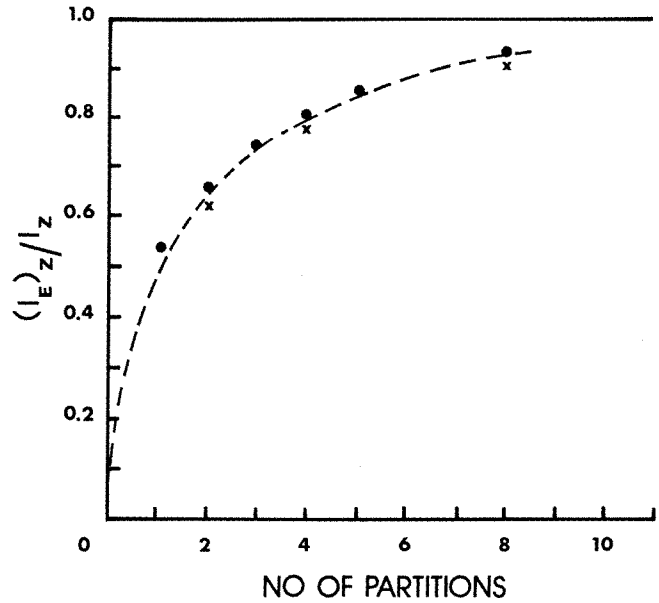

Figure 4. Relative equivalent moment of inertia around the z-axis for cylindrical containers with different numbers of partitions. Crosses: analytical solution. Points: numerical solution

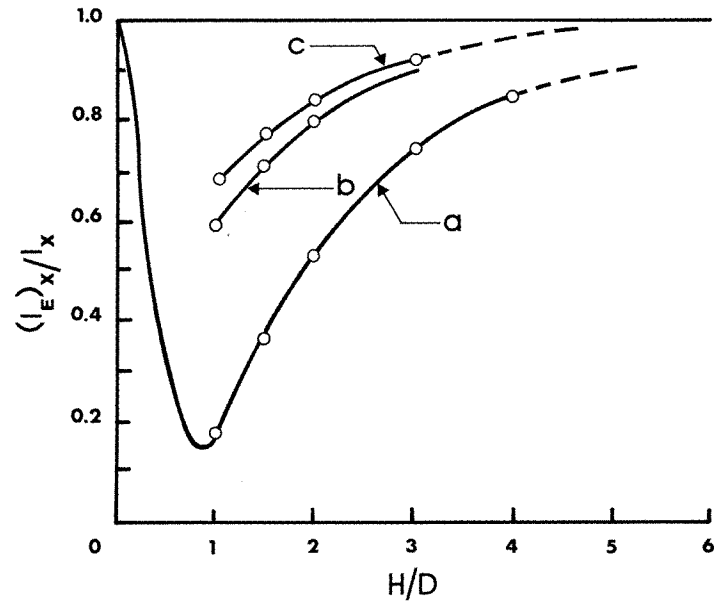

Figure 5. Relative equivalent moment of inertia for cylinders with different number of partitions as a function of aspect ratio H/D: (a) no partitions; (b) three partitions; (c) two or four partitions

Table III. Relative equivalent moment of inertia for a cylindrical container with longitudinal radial partitions rotating around the x- and y-axes

Container rotation	Number of partitions	H/D	$(I_E)_x/I_x$	$(I_E)_y/I_y$
$\gamma=(1,0,0)$	3	1	0·5784	—
		1·5	0·7113	—
		2	0·8014	—
		3	0·8934	—
$\gamma=(0,1,0)$	3	1	—	0·5874
		1·5	—	0·7113
		2	—	0·8014
		3	—	0·8938
$\gamma=(1,0,0)$	2,4	1	0·6809	—
		1·5	0·7850	—
		2	0·8546	—
		3	0·9230	—
$\gamma=(0,1,0)$	2	1	—	0·1822
		1·5	—	0·3620
		2	—	0·5389
		3	—	0·7449
$\gamma=(0,1,0)$	4	1	—	0·6809
		1·5	—	0·7850
		2	—	0·8546
		3	—	0·9230

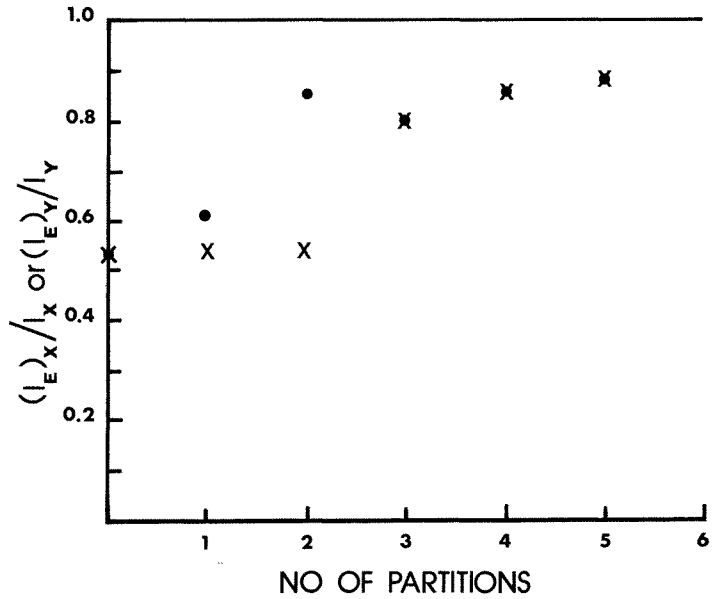

Figure 6. Relative equivalent moment of inertia around the x-axis and around the y-axis, for cylindrical containers with an aspect ratio of $H/D=2$ for different number of partitions. Points: x-axis. Crosses: y-axis

may be due to the fact that in the computation an axial rod of very small diameter was introduced in order to avoid the subdivision of the central cylindrical cell.

For the container configuration with longitudinal partitions we also performed computations where the rotation of the container was around the x- and y-axis, i.e. $\gamma = (1, 0, 0)$ and $\gamma = (0, 1, 0)$. The results are given in Table III, and in Figure 5. We see from Figure 5 that the results for three partitions lie on a different curve than those for 2 and 4 partitions.

Also, as expected, the equivalent moment of inertia for a container with partitions is higher than that for a container without partitions. In Table IV and in Figure 6 we give the results of the relative moments of inertia for a cylindrical container with an aspect ratio of $H/D = 2$ and with 1 to 5 longitudinal radial partitions around the x- and y-axes.

We see from Figure 6 that for 1 and 2 partitions $(I_E)_x \neq (I_E)_y$ whereas for 3, 4 and 5 partitions $(I_E)_x = (I_E)_y$. This is readily understandable from the tensor properties of the moment of inertia. For 3 or more partitions there are 2 or more axes of symmetry in the xy plane. The inertia tensor is therefore isotropic in the xy plane. This is not the case for the configurations with 1 and 2 partitions.

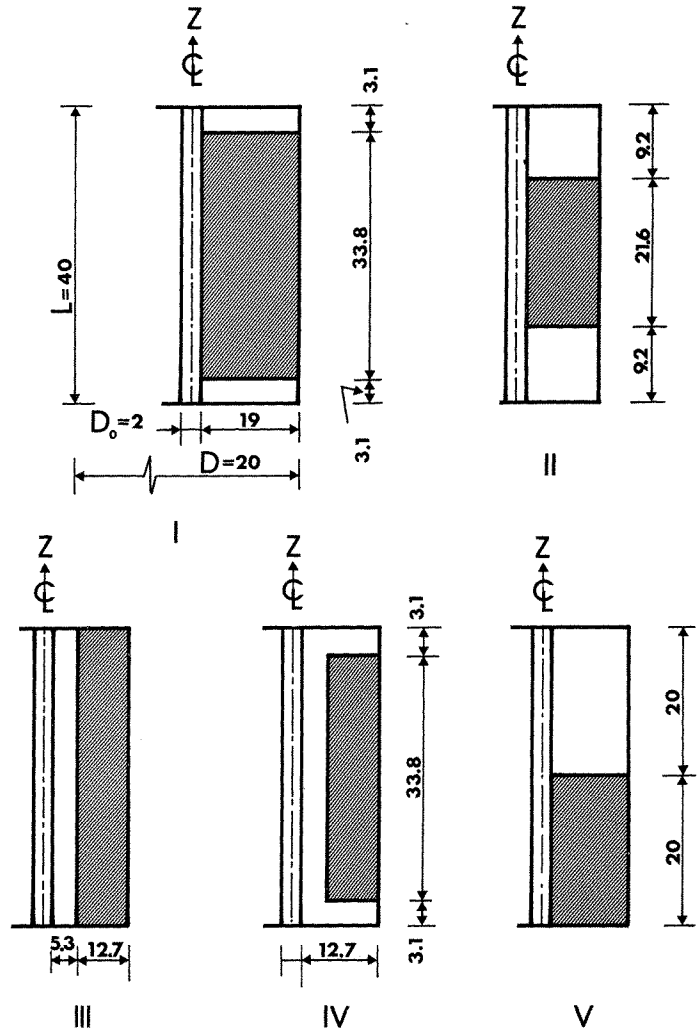

Figure 7. Geometry of partitions in the five cases with partial partitions. All dimensions are in cm

Table IV. Relative moment of inertia around the x- and y-axes for cylindrical container with $H/D = 2$ and 1 to 5 longitudinal radial partitions

Container rotation	Number of partitions	$(I_E)_x/I_x$	$(I_E)_y/I_y$
$\gamma = (1,0,0)$	1	0·6096	
	2	0·8545	
	3	0·8014	
	4	0·8546	
	5	0·8841	
$\gamma = (0,1,0)$	1		0·5389
	2		0·5389
	3		0·8014
	4		0·8546
	5		0·8841

Table V. Relative moment of inertia around x- and y-axes for a cylindrical container of aspect ratio $H/D = 2$ with 1 to 5 partial longitudinal symmetrical partitions

Case	Number of partitions	$(I_E)_x/I_x$	$(I_E)_z/I_z$
I	1	0·553	0·333
	2	0·574	0·471
	3	0·567	0·567
	4	0·574	0·631
	5	0·580	0·683
II	1	0·540	0·166
	2	0·541	0·265
	3	0·540	0·334
	4	0·541	0·380
	5	0·541	0·418
III	1	0·562	0·268
	2	0·589	0·477
	3	0·577	0·629
	4	0·589	0·727
	5	0·598	0·794
IV	1	0·544	0·196
	2	0·550	0·357
	3	0·553	0·484
	4	0·550	0·568
	5	0·553	0·635

Next we computed the equivalent moment of inertia for configurations with partial longitudinal partitions as shown in Figure 7. As seen in the Figure there were five cases of partial partitions. The number of partitions (symmetrically spaced) ranged from 1 to 5 and the aspect ratio of the container was $H/D = 2$. The results for the relative moment of inertia around the x- and y-axes for the first 4 cases are given in Table V, and plotted in Figures 8 and 9, respectively.

From Figure 8 we see that, as expected, $(I_E)_z$ for cases with partial partitions is less than that for

full partitions. What is interesting is the results for $(I_E)_x$. We see from Figure 9 that for all 4 cases of partial partitions $(I_E)_x$ is very close to what one gets for the case of no partitions. The fluid motion seems to be quite flexible in such a way that when the partitions are not full even by a small amount, the fluid behaves (in terms of the resultant moment it exerts on the container) as if they were not there at all.

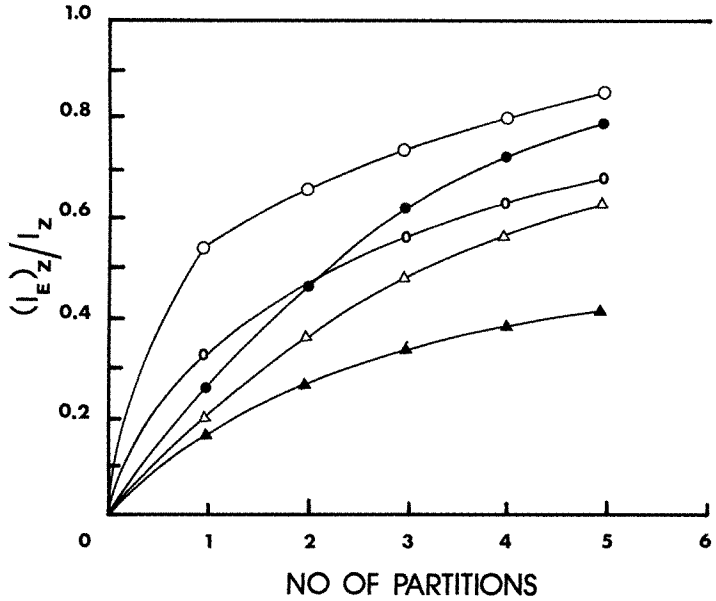

Figure 8. Relative equivalent moment of inertia around the z-axis, for cylindrical containers of aspect ratio $H/D = 2$, for different numbers of partial partitions. Open circles: full partitions. Ellipses: case 1. Full triangles: case II. Full circles: case III. Open triangles: Case IV

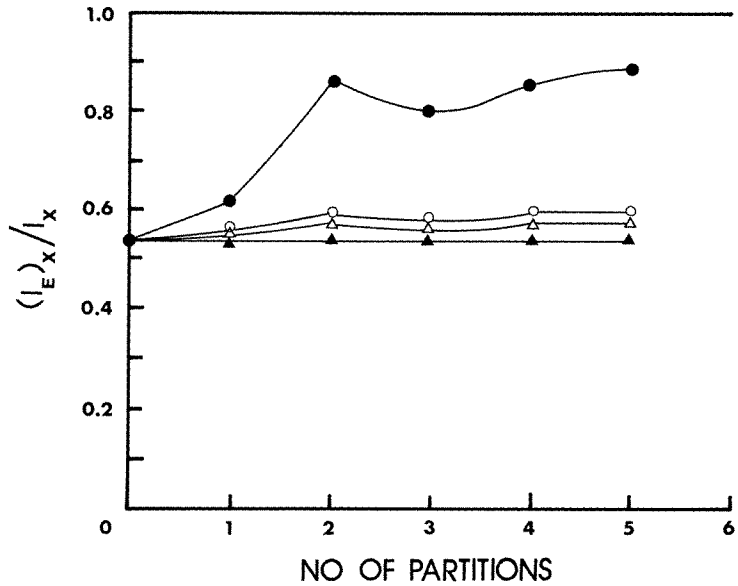

Figure 9. Relative equivalent moment of inertia around the x-axis for cylindrical containers of aspect ratio $H/D = 2$, for different numbers of partial partitions. Full circles: full partitions. Open circles: case I. Open triangles: case II. Full triangles: Case III

Table VI. Cartesian components of the resultant moments for the cylindrical container defined in Figure 7, case V, rotating with a unit angular acceleration in x, y or z direction

Container rotation	Number of partitions	M_x[dyn cm]	M_y[dyn cm]	M_z[dyn cm]
$\gamma = (1, 0, 0)$	1	$1{\cdot}135 \times 10^6$		$7{\cdot}849 \times 10^4$
	2	$1{\cdot}463 \times 10^6$		
	3	$1{\cdot}392 \times 10^6$		
	4	$1{\cdot}463 \times 10^6$		
	5	$1{\cdot}503 \times 10^6$		
$\gamma = (0, 1, 0)$	1		$1{\cdot}063 \times 10^6$	
	2		$1{\cdot}063 \times 10^6$	
	3		$1{\cdot}039 \times 10^6$	
	4		$1{\cdot}463 \times 10^6$	
	5		$1{\cdot}505 \times 10^6$	
$\gamma = (0, 0, 1)$	1	$7{\cdot}852 \times 10^4$		$1{\cdot}258 \times 10^5$
	2			$1{\cdot}779 \times 10^5$
	3			$2{\cdot}139 \times 10^5$
	4			$2{\cdot}367 \times 10^5$
	5			$2{\cdot}556 \times 10^5$

Case V differs from the first four cases in that the partitions are not symmetrical with respect to the xy plane. In Table VI we give the results for the moment components M_x, M_y and M_z obtained for rotations around the three axes.

We see from Table VI that for the case with a single partition the x- and y-axes are not the major axes of the inertia tensor, and we get $M_z \neq 0$ for $\gamma = (1, 0, 0)$ and $M_x \neq 0$ for $\gamma = (0, 0, 1)$. This means that for the case of a single partition we have a non-zero inertia product $(I_E)_{xz} = (I_E)_{zx} = -7{\cdot}85 \times 10^4\,\mathrm{g\,cm^2}$.

We used our code to compute the equivalent inertia tensor for many other container configurations with full, and partial, partitions in all three cylindrical co-ordinate directions. We assume that the results of the examples presented in this paper suffice to demonstrate the capability of the code presented.

ACKNOWLEDGEMENT

It is a pleasure to acknowledge the contribution of Prof. M. Wolfshtein in constructing the numerical scheme.

REFERENCES

1. S. Silverman and H. N. Abramson, 'Lateral sloshing in moving containers', in N. H. Abramson (Ed.) *The Dynamic Behavior of Liquids in Moving Containers*, NASA SP-106, 1966, pp. 13–78.
2. N. Ye. Zhukovskiy, *Collected Works*, Vol. 2, Gostekhizdat, 1948.
3. N. N. Moiseyev and V. V. Rumyantsev, *Dynamic Stability of Bodies Containing Fluid*, Applied Physics and Engineering. Edited by N. H. Abramson Vol. 6, Springer-Verlag, 1968.
4. Y. Kronzon, I. Partom and M. Wolfshtein, 'Numerical solution of the momentum equations in unsteady incompressible flow', in C. Taylor and B. A. Schrefler (eds), *Numerical Methods in Laminar and Turbulent Flow*, Pineridge Press, 1981, pp. 955–964.
5. N. E. Kochin *et al.*, *Theoretical Hydrodynamics*, Interscience Publishers, 1964.